Available online at www.sciencedirect.com
SCIENCE DIRECT®
International Journal of Heat and Mass Transfer 48 (2005) 3707–3712
International Journal of HEAT and MASS TRANSFER
www.elsevier.com/locate/ijhmt

Technical Note

Heat transfer due to supersonic flow impingement on a vertical plate

V. Ramanujachari [a,*], S. Vijaykant [a], R.D. Roy [a], P.M. Ghanegaonkar [b]

[a] *Institute of Armament Technology, Pune 411 025, India*
[b] *D.Y. Patil College of Engineering, Pune 411 044, India*

Received 8 August 2003; received in revised form 30 April 2004
Available online 26 May 2005

1. Introduction

Vertically launched containerized missiles have become popular in the area of medium range air defence system. The flame deflector is one of the important components of the vertical hot launch system. It is most frequently a large curved duct or plate, which performs the disposal of the exhaust gas away from the launch installations. It is required to withstand the high velocity and high temperature of the exhaust for a large number of rocket launches. Understanding the supersonic jet impingement is essential to the design of hot launch systems. Studies of momentum and heat transfer in the supersonic jet impingement are rarely found because of the complexities of interaction between shock waves and boundary layer and also because of the difficulties in measurement of the pressure and temperature on the impingement surface.

Donaldson et al. [1] conducted measurements of convective heat transfer coefficients with cold air jet impinging on a flat, circular heated plate using flush mounted calorimeter disks with thermocouples attached to them. The air velocities were varied from 60 to 210 m/s. The corresponding Reynolds numbers were in the range of 3×10^4 to 1×10^5. The distance between the nozzle exit and the plate were varied between 7 and 30 nozzle exit diameter (nozzle exit diameter = 12.5 mm). It was concluded that the stagnation point heating was relatively high compared to the wall heating at low Reynolds numbers. For high Reynolds numbers this ratio became high. At large distances from the stagnation point the heat transfer had fallen off in inverse proportion with distance. The Nusselt numbers reported were in the range of 190–500. Goldstein and Franchett [2] performed experiments to determine heat transfer to a jet of air impinging at different oblique angles (30°, 45°, 60° and 90°) to a plane surface. The jet Reynolds numbers considered were 10,000, 20,000, 30,000 and 35,000. The jet orifice to plate spacing were 4, 6 and 10 (orifice diameter = 10 mm). Contours of constant heat transfer coefficient were predicted from the isotherms obtained using temperature-sensitive liquid crystal. The Nusselt numbers obtained were in the range of 20–160. It was concluded that the location of the peak heat transfer was off-axis from the jet centerline to the plate surface for the oblique jet. The local Nusselt numbers were found to be independent of Reynolds number when divided by the Reynolds number raised to the power 0.7. Baughn and Shimizu [3] and Baughn et al. [4] carried out heat transfer studies using cold and heated air jets impinging perpendicular to a heated plate. The Reynolds numbers considered were 23,300 and 55,000. The distance between the jet exit and the impinging plate considered were 2, 6, 10 and 14 diameters (jet diameter = 26 mm). The Nusselt numbers obtained were in the range of 20–160. The conclusion of the study gave the possibility of using heat transfer data obtained from unheated jets to be used for heated jets of known effectiveness. Lee et al. [5] carried out supersonic jet impingement experiment on to an inclined plate surface (inclination angle = 45°) kept at 5 nozzle exit diameters

* Corresponding author.
E-mail address: vramanujachari@yahoo.co.in (V. Ramanujachari).

0017-9310/$ - see front matter
doi:10.1016/j.ijheatmasstransfer.2004.05.042

Nomenclature

A	cross sectional area of the slug
C	specific heat of the slug material
d	diameter of the slug
D	nozzle exit diameter
h	convective heat transfer coefficient
$J(x)$	Bessel function for x
k_g	thermal conductivity of the gas mixture
k_s	thermal conductivity of the slug material
M	mass of the slug
Nu	Nusselt number
L	length of the slug
q	heat flux
q_l	heat flux evaluated by lumped heat transfer model
r	radial coordinate
r_0	radius of the slug
T	temperature
T_0	stagnation temperature
T_s	surface temperature
x	axial distance
z	axial coordinate

Greek symbols

α	thermal diffusivity
θ	time

(diameter = 100 mm) away from the nozzle exit. The high temperature jet of Mach number 2.82, at the nozzle exit, was produced by burning a composite propellant in a rocket motor at a pressure of 89.6 bar. Twenty-five thermocouples were embedded behind the plate to obtain the temporal variation of temperature leading to the calculation of Nusselt number based on an unsteady one-dimensional heat conduction equation. The Nusselt numbers obtained were in the range of 2000–15,000 on the surface of the inclined plate. It was concluded that the Nusselt number sharply decreased with distance from the centre of the plate and the local Nusselt number of the supersonic impinging jet approached that of the subsonic jet as the distance increased.

Measurement of heat flux is vital to the design and development of systems involving combustion and heat transfer. Several types of heat flux sensors were developed in order to cater for the measurement of local convective, radiative or total heat transfer rates in missile, aircraft and launch vehicle structures [6]. Schmidt–Boelter heat flux gauge was used for heat transfer measurement in hypersonic wind tunnel, wherein the maximum stagnation temperature and heat flux were of the order of 1700 °C and 0.3 MW/m^2 respectively [7]. Gardon gauge was used to measure the heat flux under mixed convection and radiation environment [8]. The maximum temperature and heat flux measured were of the order of 700 K and 20 kW/m^2 respectively. It is clear from the literature survey that the supersonic jet impingement studies are receiving attention due to its importance in rocket technology. Also it is revealed that the heat flux gauges such as Gardon gauge and Schmidt–Boelter gauge have limited capacity for measurement of heat flux to a maximum of about 0.3 MW/m^2. As the supersonic rocket plume impingement phenomenon involves the heat flux of the order of 40 MW/m^2, the slug type heat flux gauge appears to be the only candidate. The need for the measurement of heat flux on the plume impingement region in rocket applications provided the motivation to work in this area.

The present experimental investigation is to obtain radial heat flux and Nusselt number distributions at various axial distances due to the impingement of high velocity and high temperature rocket exhaust gases generated by burning nitramine based propellant. The heat flux slug gauges are damaged due to the sudden impact pressure generated at the time of ignition at regions close to the center of the plate inline with the nozzle axis. Severe damage to the slugs is noted at axial distances less than eight nozzle exit diameters. Therefore, the static tests are carried out by keeping the vertical plate at 12–16 nozzle exit diameters from the nozzle exit plane. A valuable database has been developed. This can be used both by the numerical fluid flow modelers and structural designers of launchers.

2. Experimental investigation

Several static rocket motor firings have been carried out to obtain the heat flux distribution as a result of supersonic rocket exhaust jet impingement. The hardware set up for the experiments consists of, (i) scaled solid rocket motor mounted on a lathe bed, and (ii) a channel mount for vertical placement of impingement plate with a provision to vary the axial distance between nozzle exit and the plate. The solid rocket motor is a standard ballistic evaluation motor of inner diameter 90 mm; length 120 mm and thickness 20 mm made up of stainless steel to withstand a maximum chamber pressure of 150 bar. The impingement plate is kept vertically in front of the rocket jet exhaust at different distances in terms of nozzle exit diameters such as 12 to 16. Fig. 1

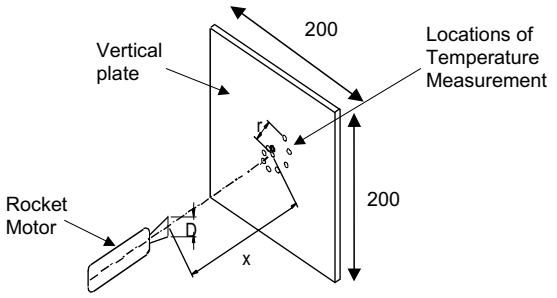

Fig. 1. Schematic of impingement plate and rocket motor.

Table 1
Experimental condition

Chamber pressure	40 bar (max)
Total temperature, T_0	3117 K
Heat capacity of the gas at chamber condition	3.1 kJ/kgK
Area ratio of the nozzle	6.4
Jet exit Mach number	3
Jet exit Reynolds number	1.69×10^5
Thermal conductivity of the gas mixture	0.025 W/mK at 300 K 0.076 W/mK at 1000 K 0.2 W/mK at 3100 K

shows the schematic of the impingement plate and the rocket motor. The exit and throat diameters of the nozzle are 24.3 mm and 9.6 mm respectively. The propellant used in this study is a nitramine based grain consisting of Nitrocellulose 54%, Nitroglycerine 39%, RDX 5% and Carbamite 2%. The inner diameter, outer diameter, length and mass of the grain are 10 mm, 66 mm, 30 mm and 165 g respectively. The composition of the products of combustion and their thermochemical properties under the conditions in Table 1 have been calculated using chemical equilibrium calculation code from Gordon and McBride [9]. The major combustion products are, CO: 31%; CO_2: 20%; H_2: 6%; H_2O: 27% and N_2: 16%. The ignition was provided by burning a pyrotechnic mixture through an electrically initiated squib.

3. Slug type heat flux gauge

Slug type heat flux gauge with necessary instrumentation lay out is shown in Fig. 2. Copper is used as the material for the slug. The dimensions are 5 mm diameter and 6 mm length. The thermal conductivity of copper is 387.6 W/mK and specific heat is 381 J/kgK. This slug is embedded in E–glass phenolic composite material plate ($100 \times 100 \times 15$ mm) to provide necessary insulation both in circumferential and axial

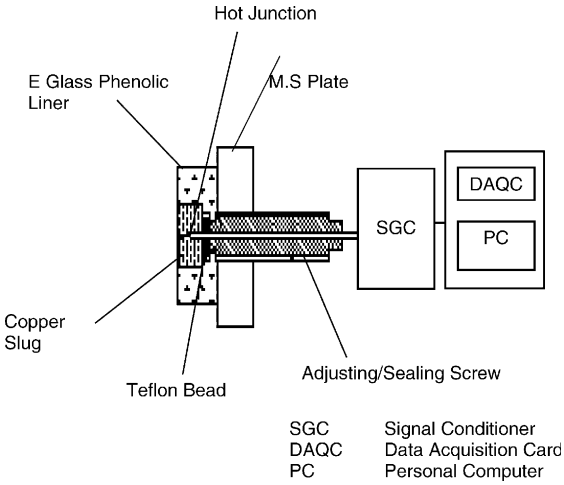

Fig. 2. Schematic of slug gauge and instrumentation.

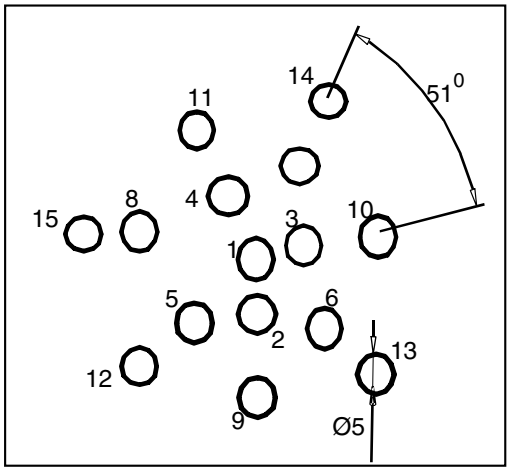

Channel	Radius (mm)
1	0.0
2	7.0
3	10.0
4	11.5
5	13.0
6	14.5
7	16.0
8	17.5
9	19.0
10	20.5
11	22.0
12	23.5
13	25.0
14	26.5
15	28.0

Fig. 3. Slug gauge arrangement on the vertical plate.

directions. A Chromel–alumel thermocouple is brazed to the copper slug by making a well in it. The thermocouple junction is at a distance of 2 mm from the exposed surface of the slug. The arrangement of the slug gauges on the vertical plate is shown in Fig. 3. In the present work, detailed unsteady axisymmetric heat conduction analysis has been carried out to find the radial distributions of temperature, heat flux and Nusselt number as explained in the next section.

4. Conduction heat transfer in slug gauge

The heat transfer in the slug gauge is based on the unsteady heat conduction in axisymmetric coordinates. The general governing equation [10] is given below:

$$\frac{\partial^2 T}{\partial r^2}+\frac{1}{r}\frac{\partial T}{\partial r}+\frac{\partial^2 T}{\partial z^2}=\frac{1}{\alpha}\frac{\partial T}{\partial \theta}. \tag{1}$$

As the jet impinges on one face of the slug when the other side and circumference are insulated by E-glass phenolic plate, the appropriate initial and boundary conditions can be formulated to solve Eq. (1). This implies that the boundary conditions are, (i) $\partial T/\partial z = 0$ at the top face ($z = L$), (ii) $\partial T/\partial r = 0$ through out the circumference of the cylinder ($r = r_0$) and (iii) variable heat flux as a function of time at $z = 0$; the initial condition being the room temperature at time, $\theta = 0$. The temperature distribution obtained by the analytical solution based on variable separable approach is given below:

$$T(r,z,\theta)=\left\{A_0(\theta)+\sum_{m=1}^{\infty}A_m(\theta)\cos m\pi z\right\}\times\left[1+\sum_{n=1}^{\infty}A_nJ_0(\lambda_n r)\mathrm{e}^{-\lambda_n^2\theta}\right]. \tag{2}$$

The constants A_0, A_m, A_n and eigenvalues λ_n are determined from the initial and boundary conditions. As the thermocouple is located along the axis of the slug gauge ($r = 0$), the second term of Eq. (2) in the square bracket becomes equal to zero. This implies that the values of A_n and λ_n are not necessary to be evaluated. A_0 and A_m have been derived for this problem considering a time varying heat flux condition at $z = 0$. Heat flux is not obtained directly from the experiments using the slug gauges. Only the temperature–time data is obtained from the experiments. This temperature–time data is utilised at first to obtain an approximate heat flux using the lumped heat transfer model i.e. $q_l=\frac{MC}{A}\left(\frac{\mathrm{d}T}{\mathrm{d}\theta}\right)$ where $(\mathrm{d}T/\mathrm{d}\theta)$ is the temporal derivative of temperature from the experimental temperature–time data during static rocket motor tests. From q_l the heat flux boundary condition for the exposed surface of the slug ($z = 0$) is obtained, namely $\left(\frac{\partial T}{\partial z}\right)_{z=0}=\frac{-q_l}{k_s}$. The temperature distribution as a function of time at $r = 0$ and $z = 2$ mm (i.e., the location of the thermocouple embedded in the slug gauge) is obtained from the analytical solution. This analytical temperature distribution is matched with the experimentally obtained temperature distribution by varying the value of $\left(\frac{\partial T}{\partial z}\right)_{z=0}$, which was initially obtained from the heat flux based on the lumped heat transfer model. The value of $\left(\frac{\partial T}{\partial z}\right)_{z=0}$, which gives a perfect matching of the experimental and analytically computed temperature profiles is used to calculate the correct value of heat flux namely $q=-k_s\left(\frac{\partial T}{\partial z}\right)_{z=0}$.

The Nusselt number can be obtained from the condition on the surface of the slug as, $q = h(T_0-T_s)$ at $z = 0$ and $Nu = hd/k_g$, where k_g is the thermal conductivity of the mixture of exhaust gases at the surface temperature, T_s. The surface temperature is estimated from Eq. (2) by substituting $z = 0$. The convective heat transfer coefficient, h is calculated for a known heat flux, q.

5. Heat flux and Nusselt number distributions

The heat flux data of five static tests are consolidated. The variation of the maximum heat flux (immaterial of the time during the static test), non-dimensionalised by the heat flux calculated at the center of the plate is plotted as a function of radial distance, non-dimensionalised by the nozzle exit diameter in Fig. 4. Except a few values, most of the heat flux values along the radial distance, at a particular axial distance, are less than the centerline value. In the midst of the data scatter, there seems to be a local maximum heat flux emerging in the radial direction of $0.5 < r/D < 1$. The discrete points are based on the analytical solution matched with the experimental temperature–time data and the continuous line is the trend line passing through majority of the scattered points. The likely cause of this scatter has been explained below.

Kim and Chang [11] reported that the impinging supersonic jet possessed complicated flow elements consisting of barrel shock, exhaust gas jet boundary, Mach disk, contact surface, reflected shock, plate shock, sub tail shock and stagnation bubble. Alvi et al. [12] also reported that the impingement region consisted of complex shock structure and high-speed radial wall jet. The measurement on the impingement region is very difficult due to high mean shear, thermal loads and unsteady pressure forces. Also, this impinging jet is accompanied by discrete, high amplitude acoustic tones, referred to as impingement tones. The fluid dynamic–acoustic interaction seems to be responsible for the scatter in the experimental data. In this case, it is not possible to separate the predominant flow elements causing this scatter. These flow elements vary with the nozzle exit conditions and the distance between the vertical plate and the nozzle exit plane. The plate shock stands just in front of the vertical plate giving rise to a low velocity region and a

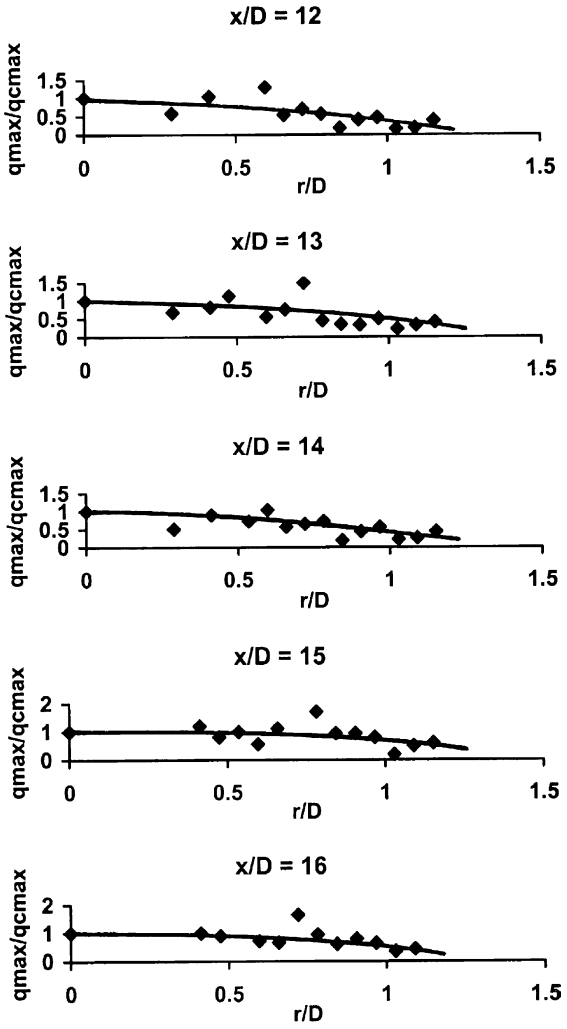

Fig. 4. Radial distribution of non-dimensional heat flux.

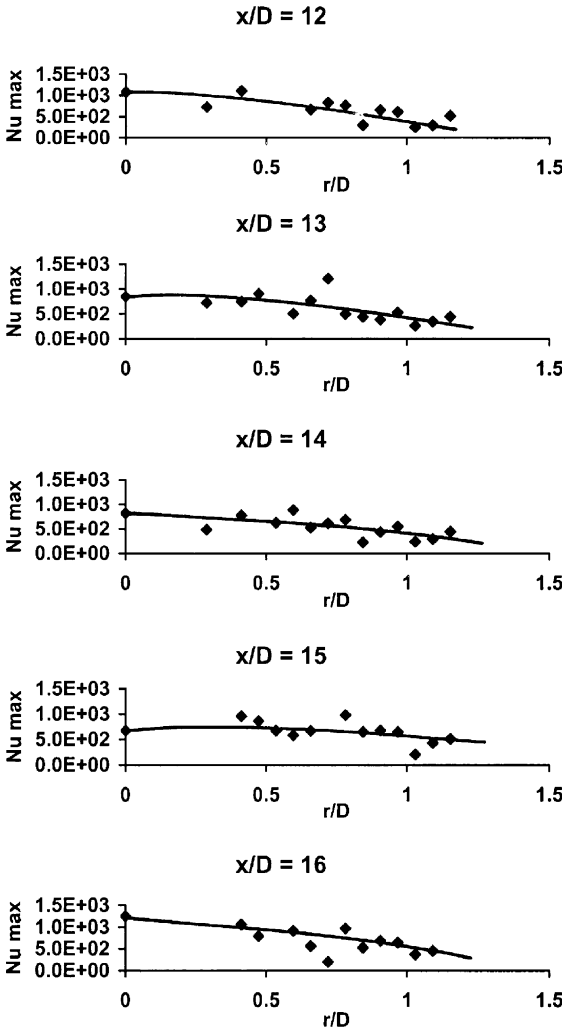

Fig. 5. Radial distribution of maximum Nusselt number.

possible stagnation bubble region ahead of the plate as reported by Kalghatgi and Hunt [13]. This is likely to increase the heat flux over a small region at the center leading to obtaining maximum heat flux at the center. In a nutshell, the $q\max/q_c\max$ vs. r/D for all the x/D values varying from 12 to 16 look almost similar.

The radial distribution of maximum Nusselt number is shown in Fig. 5 for the x/D values from 12 to 16. The variations are similar to the heat flux distributions. The maximum values of the Nusselt number and the heat flux in these cases are in the range of 900–1250 and 20–40 MW/m^2 respectively. As the situations studied are different by different researchers, a limited comparison has been attempted. The Nusselt numbers obtained at $x/D = 10$ by Donaldson et al. [1], Goldstein and Franchett [2] and Baughn et al. [4] for the subsonic impinging jets were in the range of 100–300, 20–160 and 45–145 respectively. The Nusselt number obtained in the present study at $x/D = 12$ is in the range of 250–1000, whereas, Lee et al. [5] reported 1000–8600 at $x/D = 5$ for the supersonic jets. Very high values reported by Lee et al. [5] (nearly one order of magnitude more than the values obtained in the present investigation) must have been due to the strong flow interactions in the jet impingement and wall jet regions leading to high shear stresses and gradient in shear stresses. This must have been responsible for high skin friction and wall heating leading to large heat transfer coefficients.

Lamont and Hunt [14] carried out supersonic air jet of Mach number 2.2 (nozzle exit diameter = 30 mm) impinging on a plate by varying the distances between the plate and the nozzle exit from 0.5 D to 15 D. They noted substantial changes in pressure distributions as a function of centre distance between the nozzle exit and

the plate. It was noted that the flow fields became increasingly influenced by the mixing of the jet as the distance increased until it was 15 D, where the pressure distribution took a form characteristic of a subsonic jet. The present investigation addresses the problem of supersonic jet impinging on a vertical plate kept at the distances of x/D over a range of 12–16, wherein, the influence of shock interactions decreases and the jet mixing becomes predominant. This is also indicated by the relatively low values of Nusselt number compared to the situation wherein the shock effects were predominant ($x/D = 5$) as shown by Lee et al. [5]. Though there is a scatter in the data, it is observed that there is a possibility of local maximum Nusselt number in the region of $0.5 < r/D < 1$. Baughn and Shimizu [3] obtained similar local heat transfer maximum at $r/D = 1.8$ for the x/D ratio of 2, when the subsonic jet impinges on a surface. A general conclusion can be drawn by comparing the present study with the studies conducted for the subsonic jets that the Nusselt number values for the subsonic jet is one order of magnitude less than that of the supersonic jet. The values obtained in the present investigation show that the heat transfer from the rocket plume is strongly convective in nature.

6. Conclusions

Except a few regions on the impingement plate, the stagnation point of the plate experienced the maximum heat flux based on experimental observations. The heat flux has fallen off along the radial distance in the wall jet regions. Experimental data showed a possibility of local maximum heat transfer away from the jet axis in the midst of data scatter. Comparison of the data obtained in the present investigation on supersonic jets with the data on subsonic jets reported in literature indicates that the maximum heat transfer coefficient of the supersonic jet is about one order of magnitude more than that of the subsonic jet. It is also observed based on the values of Nusselt number that the flow field has been influenced by the mixing of the jet as the distance between the plate and the nozzle exit is increased. The maximum heat flux varied between 20 and 40 MW/m^2 during these static tests. The data generated would be of immense utility to the structural designers of the flame deflectors of hot launch systems.

Acknowledgements

The authors thank Rear Admiral A.K Handa, Director & Dean, Institute of Armament Technology, Pune and Dr. V.K. Saraswat, Programme Director, PGAD, Hyderabad for their encouragement to carry out this work. The authors are indebted to Dr. Haridwar Singh, Director, HEMRL, Pune for providing solid propellant grains for conducting the tests. Thanks are due to Prof. G.C. Pant for extending facilities in the propulsion laboratory at I.A.T, Pune. The help rendered by Mr. J.C. Thomas, Mr. N.P. Mule and Mr. Anil Gawade in carrying out the experiments is sincerely acknowledged.

References

[1] C.D. Donaldson, R.S. Sneker, D.P. Margolis, A study of free jet impingement, Part 2. Free jet turbulent structure and impingement heat transfer, J. Fluid Mech. 45 (1971) 477–512.
[2] R.J. Goldstein, M.E. Franchett, Heat transfer from a flat surface to an oblique impinging jet, J. Heat Transfer 110 (1988) 84–90.
[3] J.W. Baughn, S. Shimizu, Heat transfer from a surface with uniform heat flux and an impinging jet, J. Heat Transfer 111 (1989) 1096–1098.
[4] J.W. Baughn, A.E. Hechanova, X. Yan, An experimental study of entrainment effects on the heat transfer from a flat surface to a heated circular impinging jet, J. Heat Transfer 113 (1991) 1023–1025.
[5] C. Lee, M.K. Chung, K.B. Lim, Y.S. Kang, Measurement of heat transfer from a supersonic impinging jet on to an inclined flat plate at 45°, J. Heat Transfer 113 (1991) 769–772.
[6] E.O. Doeblin, Measurement Systems: Application and Design, McGraw Hill, Tokyo, 1990.
[7] C.T. Kidd, J.C. Adams, Fast response heat flux sensor for measurement commonality in hypersonic wind tunnels, J. Spacecraft Rockets 38 (2001) 719–729.
[8] C.H. Kuo, A.R. Kulkarni, Analysis of heat flux measurement by circular foil gages in a mixed convection/radiation environment, J. Heat Transfer 113 (1991) 1037–1040.
[9] S. Gordon, B.J. McBride, Computer Program for Calculation of Complex Chemical Equilibrium Compositions, Rocket Performance, Incident and Reflected Shocks and Chapman–Jouguet Detonations, NASA SP-273, 1976.
[10] M.N. Ozisik, Heat Conduction, John Wiley and Sons, New York, 1980.
[11] K.H. Kim, K.S. Chang, Three dimensional structure of a supersonic jet impinging on an inclined plate, J. Spacecraft Rockets 31 (1994) 736–744.
[12] F.S. Alvi, J.A. Ladd, W.W. Bower, Experimental and computational investigation of supersonic impinging jets, AIAA J. 40 (2002) 599–602.
[13] G.T. Kalghatgi, B.L. Hunt, The occurrence of stagnation bubbles in supersonic jet impingement flows, Aeronaut. Quart. 27 (1976) 169–185.
[14] P.J. Lamont, B.L. Hunt, The impingement of under expanded axisymmetric jets in perpendicular and inclined flat plates, J. Fluid Mech. 100 (1980) 471–511.